Transport in magnetic multilayers from the quantum Boltzmann equation

P. B. Visscher
Department of Physics and Astronomy and Materials for Information Technology Program, University of Alabama, Tuscaloosa, Alabama 35487-0324
(Received 23 April 1993)

We describe a method for the computation of resistivity in a periodic or nonperiodic multilayer of magnetic materials. We show that the approach that leads to the well-known constant-relaxation-time solution to the Boltzmann equation in systems with spherical symmetry [J. M. Ziman, *Principles of the Theory of Solids* (Cambridge University Press, Cambridge, England, 1964)] can be generalized to cylindrical symmetry. The effects of interface scattering are included. For a layered system with a step-function potential, we have calculated scattering matrix elements from the exact quantum-mechanical wave functions. In the special case of two layers these are the well-known Kronig-Penney wave functions, but we have developed a transfer-matrix method for obtaining them in general, so our code will work for an arbitrary number of layers. We find that in realistic models there are often states trapped between high-potential layers, for which numerical divergences occur; we show how to handle these cases by a recursive procedure. The advantages of the quantum method over semiclassical ones are that (a) it includes interference effects exactly, and (b) it involves fewer free parameters. We give results for the "giant magnetoresistance" of a model of an FeCr sandwich structure for various numbers of layers. The approach to the result for an infinite periodic system is highly singular.

I. INTRODUCTION

There has recently been renewed interest in magnetic multilayers due to the discovery that several such systems exhibit a very large ("giant") magnetoresistance effect.[1] These systems consist of layers of a magnetic material (e.g., Fe) separated by layers of a nonmagnetic material (e.g., Cr). The effect occurs when there is an antiferromagnetic (AF) alignment of adjacent magnetic layers at zero field, which can be converted to a ferromagnetic (F) alignment by the application of an external field. The magnetoresistance arises because the AF configuration has a much higher resistance than the F configuration. The effect is quite robust, occurring in a number of different systems.[2] This suggests that the effect does not depend critically on the details of the band structure, but that a simple model based on free-electron-like band structures might be adequate to explain the data semiquantitatively. In this paper we present a transfer-matrix method for the calculation of quantum-mechanical wave functions in an arbitrary layered system. We calculate the scattering matrix that appears in the Boltzmann equation, and show how the Boltzmann equation may be solved to give the conductivity and magnetoresistance. We include both bulk and interface scattering mechanisms, so we can model the effects of interface scattering due to atomic-scale disorder or interdiffusion at the interface, which has been found experimentally[3] to enhance the giant magnetoresistive effect.

Resistance in layered systems has usually been studied from a semiclassical point of view (for example, the Sondheimer-Fuchs theory,[4,5] based on the Boltzmann equation). That is, the fact that electrons can be reflected or refracted by an interface between (internally uniform) materials at different potentials is taken into account through assumed reflection and transmission coefficients. This differs from our completely quantum-mechanical treatment of the problem in that it neglects interference between waves reflected at different interfaces. This neglect is justified when the layers are very thick in comparison with the electron wavelength or some quantum coherence length. However, interesting recent experimental results to which one would like to apply such a theory involve thin layers (of order 10–20 Å) for which this assumption is not justified.

Although a quantum treatment of the problem can give rise to quantum oscillations, we emphasize that this is not our reason for using a quantum approach: the rapid quantum oscillations in our system (see Figs. 4 and 5 or Ref. 10) are unlikely to be experimentally observable because they will be washed out by layer-thickness fluctuations. The lack of experimental quantum oscillations does not imply that a classical approach is adequate.

An additional practical advantage of a quantum-mechanical calculation is that it involves fewer free parameters than most semiclassical calculations. Although the reflection and transmission coefficients of a semiclassical theory can be computed quantum mechanically from the size of the potential step,[6] in most calculations they have been taken to be free parameters. If one assumes that the bulk parameters (effective mass, effective potential for electrons of each spin) are known from bulk experiments, the scattering strengths are the only free parameters in our approach.

Our calculation assumes a constant potential within each layer. Thus it does not account for details of the band structure beyond the free-electron approximation, as does, for example, the work of Herman, Sticht, and van Shilfgaarde.[7] On the other hand, it would be very difficult to calculate the resistivity in a full band-structure

0163-1829/94/49(6)/3907(9)/$06.00

calculation, as we have done for the free-electron model. Our approach is simple and efficient enough that we have been able to implement it in a menu-oriented program that runs on an IBM PC. Anyone desiring a copy of the program should contact the author.

Quantum-mechanical calculations using a Kubo formalism have been carried out by Levy and Zhang.[8] This is a very different and more abstract approach than ours. It leads to a local or nonlocal[9] conductivity from which the overall conductivity of the layered structure is obtained by integration.

In this paper we show the quantum oscillations obtained for finite FeCr sandwiches and compare them to the results for the infinite superlattice. Additional results for quantum oscillations in the superlattice have been given elsewhere.[10]

II. TRANSFER-MATRIX SOLUTION FOR WAVE FUNCTIONS IN A LAYERED SYSTEM

We will initially consider a system that is infinite in the x and y directions and periodic with period D in the z direction. The potential $V(z)$ depends only on z and is a step function, having value V_L in layer L ($L=1,2,\ldots,N$). Similarly, the effective mass is assumed equal to a constant m_L in layer L. The special case $N=2$ is the well-known Kronig-Penney[11] model. We denote the individual layer thicknesses by d_L, so that $D=d_1+d_2+\cdots+d_N$. The wave functions in such a system have the Bloch form

$$\psi(z)\exp(ik_x x+ik_y y)\ , \tag{1}$$

where $\psi(z)$ satisfies a one-dimensional (1D) Schrödinger equation and the Bloch condition

$$\psi(z+D)=\exp(ik_z D)\psi(z) \tag{2}$$

for some k_z. The Brillouin zone is infinite in the x and y directions, and of width $2\pi/D$ in k_z. Within layer L, the solution $\psi(z)$ is a linear combination of sin and $\cos(k_L z)$, where k_L is defined by

$$\hbar^2(k_L^2+k_x^2+k_y^2)/2m_L+V_L=\epsilon\ , \tag{3}$$

and ϵ is the energy eigenvalue.

In the familiar 1D potential-barrier problem, the effective mass is the same on both sides, and the appropriate boundary conditions are that ψ and $d\psi/dz$ are continuous. Thus the momentum density $\psi^* d\psi/dz$ is continuous. When the materials are different, we must be more careful. We will still assume ψ continuous, but physically it is the normal mass flux $\psi^*(\hbar/m)d\psi/dz$ (for a plane wave, this is $v|\psi|^2$ where $v=\hbar k/m$) rather than the momentum density that must be continuous. Thus we should assume continuity of $(\hbar/m)d\psi/dz$ instead of $d\psi/dz$ itself. (This result can also be derived by looking at the layered free-electron system as the long-wavelength limit of a tight-binding system, in which the overlap integral, which controls the effective mass, is different in different layers.)

To find the wave function, we need to pick two complex coefficients in each layer, such that the values of ψ and $v\equiv(\hbar/m)d\psi/dz$ are continuous at the interlayer boundaries. To do this, note that ψ and v at $z=0$ are linearly related to the two coefficients and therefore to ψ and v at each other point z within the same layer. A little algebra allows this relationship to be written

$$\Psi(z)=M_L\Psi(0)\ , \tag{4}$$

where the column vector Ψ is

$$\Psi\equiv\begin{pmatrix}\psi\\(\hbar/m)d\psi/dz\end{pmatrix} \tag{5}$$

and the matrix M_L is

$$M_L\equiv\begin{pmatrix}\cos kz & v^{-1}\sin kz\\ -v\sin kz & \cos kz\end{pmatrix}\ , \tag{6}$$

where we have written k for k_L and v for $\hbar k_L/m$. Note that Eq. (6) holds for imaginary as well as real k. To compute it numerically in the imaginary case, when $k^2<0$ we define a positive real $\tilde{k}$ so that $k=i\tilde{k}$ and $\tilde{v}=\hbar\tilde{k}/m$, and use

$$M_L\equiv\begin{pmatrix}\cosh\tilde{k}z & \tilde{v}^{-1}\sinh\tilde{k}z\\ \tilde{v}\sinh\tilde{k}z & \cosh\tilde{k}z\end{pmatrix}\ . \tag{7}$$

In what follows we will put $z=d_L$ in Eq. (6) so that M_L can be thought of as a transfer matrix that gives the wave function at the right side of a layer in terms of that at the left. Using Eq. (4) N times to propagate across all the layers, the Bloch condition [Eq. (2)] becomes

$$M\Psi=\exp(ik_z D)\Psi\ , \tag{8}$$

where

$$M\equiv M_N\cdots M_2 M_1\ . \tag{9}$$

The eigenvalue equation [Eq. (8)] has a solution if and only if the determinant of $M-\exp(ik_z D)$ vanishes. Using the fact that M_L and therefore M have unit determinant, this condition is easily converted to

$$\cos k_z D=\tfrac{1}{2}\,\mathrm{tr}M\ . \tag{10}$$

Thus our transfer-matrix method leads to a simple explicit formula for k_z. Since k_L [Eq. (3)] depends only on

$$k_r=(k_x^2+k_y^2)^{1/2}\ , \tag{11}$$

the Fermi surface is a surface of revolution, and we need only plot a cross section, i.e., a graph of k_z vs k_r, as in Fig. 1 below. For a given k_r, if Eq. (10) is between -1 and 1, there is a solution for k_z and a point of the Fermi surface; if not, k_r lies in a gap between sheets. In the former case, it is easy to solve Eq. (8) for $\Psi(0)$ and use Eq. (4) to find the wave function $\psi(z)$ everywhere (Fig. 2 below).

To calculate the conductivity, which is an integral over the Fermi surface, we require a sampling of points on the Fermi surface. It is not sufficient to use an evenly spaced grid in k_r, because near $k_z=0$ and $k_z=\pi/D$, the slope $\partial k_z/\partial k_r$ diverges, requiring very closely spaced k_r. We use an algorithm that chooses the increments dk_r so that

the areas of the resulting pieces of Fermi surface are approximately equal. In a gap between sheets, we use an interpolative search procedure based on Newton's method to find the edge of the next sheet.

III. FERMI SURFACES FOR FeCr SUPERLATTICES; TRAPPED STATES

In a free-electron model of a real material, the electron density $N=(2\pi)^{-3}(4\pi/3)k_F^3$ represents the density of itinerant electrons, moving in a weak pseudopotential determined by the core potentials and the electrons bound in the cores. Thus the number of itinerant electrons per atom need not be an integer—these plane-wave states may include admixtures of both s- and d-like orbitals. The lattice (with core electrons) must have a positive charge (assumed uniformly distributed) of equal magnitude. To model an FeCr structure we need to choose three potentials $V_{\mathrm{Fe}+}$, $V_{\mathrm{Fe}-}$, and V_{Cr}, where + and − refer to the spin directions. We have taken the relative values of these V's from the work of Inoue, Oguri, and Maekawa:[12] relative to the mean Fe potential, these are $V_{\mathrm{Fe}\pm}=\pm 0.81$ eV, $V_{\mathrm{Cr}}=0.56$ eV. To set the absolute levels (i.e., the Fermi energy ϵ_F), we have chosen $N_{\mathrm{Fe}+}$ to be 2 electrons/atom = 30 Å^{-3}. This gives $k_F=1.93$ Å^{-1} and (setting the energy origin at $\epsilon_F=\hbar^2k_F^2/2m^*$) $V_{\mathrm{Fe}+}=-3.72U=-3.52$ eV, in terms of a convenient energy unit

$$U=(\hbar^2/2m^*)\ \text{Å}^{-2}=0.946\ \text{eV}\ , \tag{12}$$

where we have taken the effective mass m^* to be the same for all layers and equal to 4.0 times the free-electron mass. We specify energies in U rather than in eV because our MR results depend only on V_L/U; they can be applied to models with different effective masses by simply scaling all energies by U. The resulting values of all the potentials are given in Sec. V below (Table I).

The overall electron density in our layered system is not simply related to the choice of potential, and in general the densities of the F and AF configurations will be different. In principle we should adjust the Fermi energy for each configuration, because physically these densities must of course be the same. However, we have checked that these differences are negligible (less than one part in 10^4) and do not affect our conclusions about the MR.

We show in Fig. 1 the Fermi surfaces (FS) resulting from these potentials for an infinite periodic system of alternating Fe and Cr layers of thickness $d=3$ Å. The left-hand (low k_r) sheets in Fig. 1 resemble the free-electron case, for which each FS sheet would be a slice of a sphere cut by horizontal planes separated by $2\pi/D$. We show in Fig. 2 the wave function at the point labeled "2" in the minority-spin ferromagnetic FS, Fig. 1(b).

The nonconstancy of the potential is important only near the Brillouin-zone boundaries, where it introduces a gap between otherwise-degenerate sheets. For a given energy ϵ [Eq. (3)], this effect is greatest for large k_r (i.e., large kinetic energy parallel to the layers) because then the remaining kinetic energy (perpendicular to the layers)

$$\epsilon_z\equiv\hbar^2k_L^2/2m \tag{13}$$

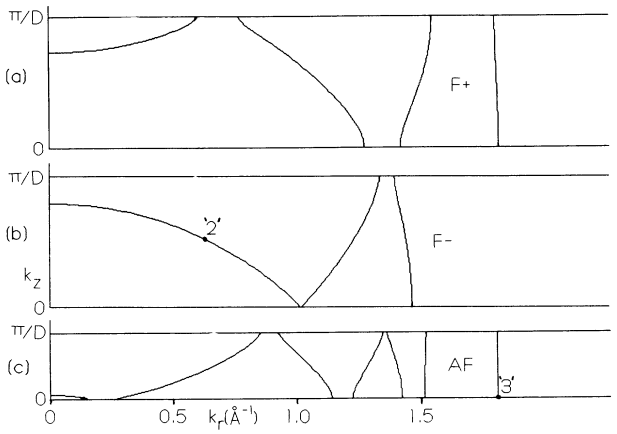

FIG. 1. Cross sections of the Fermi surfaces (FS) of a periodic FeCr superlattice for (a) majority and (b) minority spin electrons in the ferromagnetic configuration, and (c) either carrier in the antiferromagnetic configuration, using layer thickness $d=3$ Å. Each FS sheet is a solid of revolution about the vertical (k_z) axis. Only the top half of the Brillouin zone (from $k=0$ to π/D) is shown. Note that the periodicity D is larger ($D=4d$) for the antiferromagnetic case than for the ferromagnetic ($D=2d$) case. In the repeated zone scheme, the leftmost sheet of each FS is a "lens" and the other pieces are undulating cylinders. This figure (as well as Figs. 2 and 3) is an annotated screen dump from the PC program mentioned in Sec. I.

may be comparable to or smaller than the potential step V_1-V_2. We show in Fig. 3 the wave function for the state marked "3" in Fig. 1, as well as the potential $V(z)$. The wave function is effectively trapped in the lowest-potential layer.

The trapped states pose the most serious numerical problem in computing band structures of realistic layered systems. This is clear from Eq. (7), which diverges as

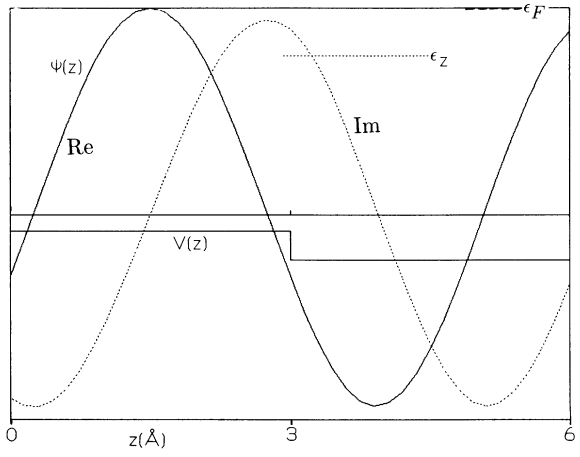

FIG. 2. The wave function $\psi(z)$ at the point ($k_r=0.663$ Å^{-1}) labeled "2" in Fig. 1(b). The solid and dashed curves are the real and imaginary parts, respectively. The potential is also shown, on an arbitrary scale, with ϵ_F (top of graph) and the perpendicular kinetic energy ϵ_z [Eq. (13)] indicated. Because $\epsilon_z \gg |V_{\mathrm{Cr}}-V_{\mathrm{Fe}-}|$, ψ is quite free-electron-like.

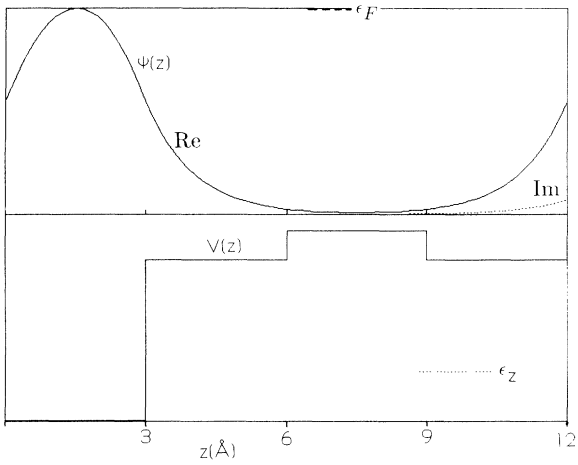

FIG. 3. The wave function at the point labeled "3" in Fig. 1(c). Notation is as in Fig. 2. Because $\epsilon_z \ll V(z)$ in the barrier layers, the wave function is trapped.

$\exp(\tilde{k}d_L)$ with increasing d_L. Eventually numerical overflow will occur, but a more immediate problem is that the trace in Eq. (10) varies extremely rapidly with k_r, making interpolative solution impossible. The rightmost sheet of FS becomes nearly vertical in Fig. 1, i.e., it is nearly a cylinder. It can be seen from Fig. 3 that trapping occurs for large k_r when d_L is only a few Angstrom units.[10] For these values of k_r, we must treat the system as finite rather than periodic, with decaying-exponential boundary conditions; then the corresponding sheet of Fermi surface is exactly cylindrical. If the electron is trapped in a "channel" between layers L and L', the boundary condition at the right edge of layer L (the left edge of the channel) states that the column vector [Eq. (5)] there must be proportional to

$$\begin{bmatrix} 1 \\ \hbar\tilde{k}/m \end{bmatrix} .$$

Applying the matrix

$$M \equiv M_{L'-1} \cdots M_{L+1} \tag{14}$$

must give a similar column vector at the left edge of layer L', which is orthogonal to the row vector

$$(\hbar\tilde{k}/m \quad 1)$$

so that

$$(\hbar\tilde{k}/m \quad 1)M \begin{bmatrix} 1 \\ \hbar\tilde{k}/m \end{bmatrix} = 0 \tag{15}$$

is the condition for a bound state, analogous to Eq. (10) for a band state. We use the same interpolative search procedure mentioned above for finding the band edge (solving $\frac{1}{2}\,\mathrm{tr}M = \pm 1$) to solve Eq. (15).

Unfortunately, Eq. (15) can still diverge, since it involves the matrices M_L just as Eq. (10) did. This will occur when a layer *inside* the channel becomes a barrier (has large M_L), thus dividing the channel into two. Then each of these channels can subdivide, and so on. Writing a code to handle all such possibilities for an arbitrary number of layers is not trivial. However, we have found that the problem can be solved quite generally by using a recursive procedure to compute all the bound states in a channel. It increases k_r until some element of the matrix M exceeds a preset limit, indicating channel subdivision, at which point it calls itself twice to compute all the remaining bound states in each subchannel. This can continue to an arbitrary depth of recursion.

IV. SEMICLASSICAL TRANSPORT IN CYLINDRICAL SYMMETRY

Since our layered system is invariant under rotations about the z axis, the problem has cylindrical symmetry in k space. Each sheet of the Fermi surface is a surface of revolution about the k_z axis. We will calculate steady-state transport in this system using the linearized semiclassical Boltzmann equation. That is, we assume the system is characterized by a steady-state distribution function $f_{\mathbf{k}} = f^0(\epsilon_{\mathbf{k}}) + g_{\mathbf{k}'}$ where $f^0(\epsilon)$ is the equilibrium Fermi-Dirac distribution function at temperature T. The Boltzmann equation has the form[13]

$$\mathbf{v}_{\mathbf{k}} \cdot e\mathbf{E}\partial f^0/\partial\epsilon = \int (g_{\mathbf{k}'} - g_{\mathbf{k}}) Q(\mathbf{k},\mathbf{k}') d^3k' , \tag{16}$$

where $Q\, d^3k'$ is the probability (per unit time) of scattering to state $\mathbf{k}$ from a state in the volume element d^3k' near $\mathbf{k}'$ (or vice versa, since we assume elastic scattering here), $\mathbf{E}$ is the electric field, and the velocity $\mathbf{v}_k$ is $\hbar^{-1}\partial\epsilon/\partial k$.

The most common application of Eq. (16) involves the use of the constant-relaxation-time approximation, in which the scattering term [the right-hand side of Eq. (16)] is assumed to be $-g_{\mathbf{k}}/\tau$. This leads to

$$g_{\mathbf{k}} = -\tau \mathbf{v}_{\mathbf{k}} \cdot e\mathbf{E}\partial f^0/\partial\epsilon . \tag{17}$$

It is well known[13] that if one assumes spherical symmetry for the unperturbed system, the constant-relaxation-time-approximation distribution function [Eq. (17)] is an exact solution of the Boltzmann equation, for some τ. We would like to generalize this result to lower (cylindrical) symmetry. We will begin by giving a version of the standard derivation that makes it clear how the symmetry is involved. Essentially, the spherical symmetry determines the angular dependence of $g_{\mathbf{k}}$. We adopt the ansatz that $g_{\mathbf{k}}$ is proportional to the cosine of the angle between $\mathbf{k}$ and $\mathbf{E}$:

$$g_{\mathbf{k}} = \gamma(k)\mathbf{E}\cdot\mathbf{k} , \tag{18}$$

where the "distribution factor" $\gamma(k)$ depends only on the magnitude of k. Substituting this into the Boltzmann equation [Eq. (16)], one encounters the integral

$$\int \gamma(k') Q(\mathbf{k},\mathbf{k}') \mathbf{k}' d^3k' . \tag{19}$$

Spherical symmetry implies that this integral must point along $\mathbf{k}$; denote it by $A(\gamma,k)\,\mathbf{k}$ (it is a linear functional of the distribution factor γ).[14] Symmetry also requires that the velocity point along $\mathbf{k}$, i.e., $\mathbf{v} = v\mathbf{k}/k$. Thus each term of the Boltzmann equation [Eq. (16)] is proportional to

$\mathbf{E}\cdot\mathbf{k}$; canceling this, it becomes

$$k^{-1}v_k e\partial f^0/\partial\epsilon = A(\gamma,k)-R(k)\gamma(k)\ , \tag{20}$$

where

$$R(k)\equiv\int Q(\mathbf{k},\mathbf{k}')d^3k' \tag{21}$$

is a rate for scattering out of state $\mathbf{k}$. Now that we have removed the angle dependence, Eq. (20) is a straightforward integral equation for $\gamma(k)$, and by finding a solution we will validate our initial ansatz about the angular dependence of $g_{\mathbf{k}}$. If we assume temperature $T=0$, so $\partial f^0/\partial\epsilon$ is a Dirac δ function $-\delta(\epsilon-\epsilon_F)$ at the Fermi surface, we can assume $\gamma(k)=\gamma_1\delta(\epsilon-\epsilon_F)$ as well, and Eq. (20) can be solved trivially. The resulting distribution function is exactly of the form of Eq. (17) with the usual result[13]

$$\tau^{-1}\equiv\int Q(\mathbf{k},\mathbf{k}')(1-\mathbf{k}'\cdot\mathbf{k}/k^2)d^3k' \tag{22}$$

for the relaxation time.

We will now generalize this derivation to the case of cylindrical symmetry. In general the electric field will have components both along and perpendicular to the z axis. Since $g_{\mathbf{k}}$ depends linearly on $\mathbf{E}$, we can treat these cases separately and superpose the results. We will first consider the case of most experimental interest, in which $\mathbf{E}$ is in the layer plane ($E_z=0$). We will again use the ansatz [Eq. (18)], but now the distribution factor γ may depend on both the radial and axial components k_r and k_z; it is independent only of the azimuthal angle ϕ. Symmetry now requires only that the integral [Eq. (19)] has the same azimuthal angle as $\mathbf{k}$; it need not point along $\mathbf{k}$. But its z component is irrelevant, so we will consider only the in-plane component

$$\int\gamma(k')Q(\mathbf{k},\mathbf{k}')\mathbf{k}_r'd^3k' \tag{23}$$

where $\mathbf{k}_r$ is the in-plane ("radial") component of $\mathbf{k}=\mathbf{k}_r+k_z\hat{\mathbf{z}}$. Then the integral [Eq. (23)] must point along $\mathbf{k}_r$, and we can write it as $A(\gamma,k_r,k_z)\mathbf{k}_r$. Cylindrical symmetry also requires the in-plane component of the velocity $\mathbf{v}_{\mathbf{k}}$ to point along $\mathbf{k}_r$, so we can write it as $v_r(k_r,k_z)\mathbf{k}_r/k_r$. Then we can again cancel $\mathbf{E}\cdot\mathbf{k}_r$ from the Boltzmann equation [Eq. (16)], leaving

$$k_r^{-1}v_r e\partial f^0/\partial\epsilon = A(\gamma,k_r,k_z)-R(k_r,k_z)\gamma(k_r,k_z) \tag{24}$$

which has no ϕ dependence. The only difference between this and the spherical-symmetry case is that the points of the Fermi surface (a curve in the k_r-k_z plane) are not equivalent, so that even at $T=0$, we must in general solve a nontrivial integral equation for γ. This is a relatively straightforward numerical problem, but for the case of δ-function scatterers considered in this paper, we will see that it turns out to be unnecessary; A is identically zero, so we can solve for γ by just dividing by R.

After finding γ, we can obtain the conductivity in the usual way.[13] Using $\mathbf{j}=(2\pi)^{-3}e\int g_{\mathbf{k}}\mathbf{v}_{\mathbf{k}}d^3k$ and $\mathbf{j}=\sigma\mathbf{E}$, the in-plane conductivity tensor is

$$\sigma=(2\pi)^{-3}e\int\gamma\mathbf{v}_r\mathbf{k}_r d^3k\ . \tag{25}$$

We now need to compute the scattering probability per unit time, $Q(\mathbf{k},\mathbf{k}')d^2k'$. For scattering from a static potential V, Fermi's Golden Rule[15] gives

$$Q(\mathbf{k},\mathbf{k}')d^3k'=2\pi\hbar^{-1}|V_{\mathbf{k}\mathbf{k}'}|^2\Omega\,dN(\epsilon)\ , \tag{26}$$

where $V_{\mathbf{k}\mathbf{k}'}$ is the matrix element of the scattering potential between states $\mathbf{k}$ and $\mathbf{k}'$. Here $\Omega\,dN(\epsilon)$ denotes the number of states per unit energy at the energy $\epsilon_{k'}$ in the volume element d^3k' near $\mathbf{k}'$; it is proportional to the volume Ω of a normalization box. Because these states lie near a constant-energy surface, it is best to coordinatize k space using a variable $k_\perp$ perpendicular to this surface and area element dk_{FS} in the surface, so that a cylindrical volume element of height $dk_\perp$ and base dk_{FS} contains the states within dE of ϵ_k where $dE=(\partial E/\partial k_\perp)dk_\perp=\hbar v dk_\perp$. Then we find

$$dN(\epsilon)=(2\pi)^{-3}dk_{\mathrm{FS}}/\hbar v \tag{27}$$

and the total density of states per unit volume is just $\int dN(\epsilon)$, integrated over a constant-energy surface.

We will now calculate the matrix element $V_{\mathbf{k}\mathbf{k}'}$. In this paper we will consider the case that the scatterers are of negligible extent (δ functions). We will assume that the scattering potential of a scatterer at $\mathbf{r}_{\mathrm{sc}}$ has the form

$$V(\mathbf{r})=V_0\delta(\mathbf{r}-\mathbf{r}_{\mathrm{sc}})\ . \tag{28}$$

We will normalize the wave function ψ so that the total wave function is

$$\Omega^{-1/2}\exp(ik_x x+ik_y y)\psi_{\mathbf{k}}(z)\ , \tag{29}$$

so that the scattering matrix element is

$$V_{\mathbf{k}\mathbf{k}'}=V_0\Omega^{-1}|\psi_{\mathbf{k}}^*(z_{\mathrm{SC}})\psi_{\mathbf{k}'}(z_{\mathrm{SC}})| \tag{30}$$

and is independent of the x and y coordinates of the scatterer. The important feature of this matrix element from the point of view of transport calculations is that it does not depend on the azimuthal angle ϕ' of $\mathbf{k}'$.

We can allow any combination of bulk and surface scatterers, with both spin-dependent and spin-independent strengths V_0. We denote the volume density of bulk scatterers in layer L by ρ_L^b. We label an interface by I and refer to its position as z_I and to the surface density of scatterers there by ρ_I^i. Then it is easy to average Eq. (26) over the positions of the scatterers (assumed to scatter incoherently) to get

$$Q(\mathbf{k},\mathbf{k}')d^3k'=2\pi\hbar^{-1}V_0^2D^{-1}dN(\epsilon)\times\left[\sum_I\rho_I^i|\psi_{\mathbf{k}}^*(z_I)\psi_{\mathbf{k}'}(z_I)|^2+\sum_L\rho_L^b\int_0^D|\psi_{\mathbf{k}}^*(z)\psi_{\mathbf{k}'}(z)|^2dz\right]\ . \tag{31}$$

This result can now be integrated [Eq. (21), which is now an integral over the Fermi surface] to give the relaxation rate R.

Because Q does not depend on the azimuthal angle ϕ' of $\mathbf{k}'$, the angular dependence of the integrand in Eq. (23)

is cos ϕ', and the integral over ϕ' is zero. Thus A is zero in Eq. (24), and we obtain immediately

$$\gamma(k_r,k_z)=-R^{-1}k_r^{-1}v_r e\partial f^0/\partial\epsilon \ . \tag{32}$$

Note that R^{-1} plays the role of a relaxation time in this δ-function scattering case [the $\mathbf{k}'\cdot\mathbf{k}$ term in Eq. (22) vanishes, making it identical with Eq. (21)]; we will denote R^{-1} by τ below. We can now substitute γ into Eq. (25) for the conductivity. It is isotropic in the layer plane, so we need only calculate the xx component. Writing $d^3k=d^2k_{\rm FS}dk_\perp$ and noting that $\int dk_\perp \partial f^0/\partial\epsilon=-1/\hbar v$ over any interval of $k_\perp$ cutting the Fermi surface, we get

$$\sigma=\sigma_{xx}=(2\pi)^{-3}e^2\hbar^{-1}\int (v_r v_x k_x\tau/k_r v)d^2k_{\rm FS} \ . \tag{33}$$

To do the angular integral, we write $d^2k_{\rm FS}=k_r d\phi\, dk_\parallel$ where $dk_\parallel$ is a length increment along the Fermi-surface curve in the k_r-k_z plane. Using $k_x=k_r\cos\phi$ and $v_x=v_r\cos\phi$, we obtain finally

$$\sigma=(2\pi)^{-3}e^2\hbar^{-1}\int (v_r^2\tau/v)\pi k_r dk_\parallel \ . \tag{34}$$

To evaluate this conductivity numerically we must calculate $\mathbf{v}$ at each point of the Fermi surface. The component v_z perpendicular to the planes is given by

$$\hbar v_z=\partial E/\partial k_z=\frac{\partial(\mathrm{tr}M)/\partial k_z}{\partial(\mathrm{tr}M)/\partial E} \ , \tag{35}$$

where

$$\partial(\mathrm{tr}M)/\partial k_z=-2\cos k_z D$$

from Eq. (10) and

$$\partial(\mathrm{tr}M)/\partial E=\sum_L \partial(\mathrm{tr}M)/\partial k_L(\partial k_L/\partial E) \tag{36}$$

which can be evaluated from Eqs. (3), (7), and (9). The other velocity component is defined by a derivative at constant k_z,

$$\hbar v_r=\partial E/\partial k_r \ . \tag{37}$$

But k_z depends on the k_L's in the layers, and if all the effective masses m_L are the same, these k_L's can be held constant by varying ϵ and k_r so that Eq. (3) remains true. Differentiating Eq. (3) gives

$$(\hbar^2/m)k_r dk_r=dE$$

(where m is the common effective mass) so that we obtain the free-electron-like result

$$v_r=\hbar k_r/m \ . \tag{38}$$

This result has an interesting consequence for the magneto-resistance, which we will describe below. It does not appear that Eq. (38) is true when the effective masses are different, or for systems without cylindrical symmetry; in general v_r must be evaluated from an equation similar to Eq. (35).

Now we can evaluate the conductivity numerically from Eq. (34) in the course of plotting the Fermi surface shown in Fig. 1. In a magnetic system, we do the FS and conductivity calculations separately for the minority and majority spins. We will show some results for magnetoresistance in the next section.

There is an interesting special relation between the conductivity and the total electron density, valid in the case of cylindrical symmetry, resulting from the special free-electron-like v_r. To see this, note that a coin-shaped volume element of the interior of the FS is $d^3k=\pi\mathbf{k}_r^2 dk_z$. The vertical height dk_z is related to the slant height by $dk_z/dk_\parallel=v_r/v$, leading to

$$\sigma=(2\pi)^{-3}e^2\hbar^{-1}\int (v_r/k_r)\tau d^3k \ . \tag{39}$$

But because of the special free-electron result [Eq. (39)], the ratio in the integrand is a constant, $\hbar/m$. If τ is also constant, the integral is just proportional to the electron density and we recover the Drude result $\sigma=ne^2\tau/m$. This is true in both the ferromagnetic and antiferromagnetic configurations in a giant-magnetoresistance system, so since the total electron density is the same in both configurations, the conductivity is as well. We conclude that the magnetoresistance (parallel to the layers) vanishes if the relaxation time and effective mass are constant. This result has been observed independently by Levy.[16]

We can also calculate the conductivity in the z direction, perpendicular to the layer planes. In this case the left-hand side of the Boltzmann equation [Eq. (16)] has no angular dependence, so the consistent ansatz is that $g_{\mathbf{k}}$ depends only on k_r and k_z:

$$v_z e\partial f^0/\partial\epsilon=A'(g,k_r,k_z)-R(k_r,k_z)g(k_r,k_z) \ , \tag{40}$$

where

$$A'\equiv\int \gamma(k')Q(\mathbf{k},\mathbf{k}')d^3k' \ . \tag{41}$$

In this case, A' does *not* vanish for δ-function scatterers, so one must solve an integral equation to get the perpendicular conductivity.

Parts of a formal development using the same general viewpoint as the present one were described by Inoue, Oguri, and Maekawa[17] for a two-layer system (Kronig-Penney model). This differed from the present work in that they did not calculate any wave functions (they used $\psi=1$), and their numerical results did not depend on the quantum-mechanical nature of the model.

V. RESULTS

Magnetoresistances resulting from applying the method described here to infinite FeCr superlattice structures have been given elsewhere;[10] we will give here MR results for finite sandwich structures to see how the infinite limit is approached. We summarize in Table I the parameter values we have used.

The scattering parameters $S_{\rm bulk}$ and $S_{\rm sd}$ in Table I are defined as follows. The scattering probability due to interface I in Eq. (31) is proportional to $V_0^2\rho_I^i$. Assuming this is due to interface roughness, the scattering centers are atoms situated on the wrong side of the interface; the perturbation to the potential at such an impurity site is the difference between the atomic potentials of the two materials. Within our step-potential model, this is just

TABLE I. The parameters used, in terms of the energy unit U [Eq. (12)] and in electron volts. Only the relative values of the scattering strengths S affect the MR.

m^*	$4m_e$	
V_{Fe+}	$-3.71\ U$	-3.515 eV
V_{Fe-}	$-2.00\ U$	-1.896 eV
V_{Cr}	$-2.27\ U$	-2.148 eV
S_{sd}	1.0 Å^{-2} (scattering, spin-dependent)	
S_{bulk}	$0.4U^2$ Å^{-3}	0.358 (eV)^2 Å^{-3}
Δ	0.0125 (convergence parameter; see Appendix)	

the potential jump ΔV_I at a step I. Allowing also for interface scattering due to impurities or lattice defects, which does not depend on the potential difference, we thus parametrize the interface scattering by

$$V_0^2\rho_I^i = S_{si} + S_{sd}(\Delta V_I)^2 \ . \tag{42}$$

For notational consistency, we parametrize the bulk scattering by

$$V_0^2\rho_L^b = S_{bulk} \tag{43}$$

so that the free parameters S_{si}, S_{sd}, and S_{bulk} control the spin-independent, spin-dependent, and bulk scattering respectively. We have shown previously[10] that large magnetoresistances are obtained only when spin-dependent scattering is included, so in this paper we will concentrate on this case. A small S_{bulk} must be included to avoid infinite relaxation times when ψ vanishes accidentally at interfaces, but we have approximated the corresponding term in Eq. (31) using $\psi=1$. The exact ψ was used in the interface term.

We have defined the magnetoresistance by

$$\mathrm{MR} \equiv \frac{1/\sigma(\mathrm{F}) - 1/\sigma(\mathrm{AF})}{1/\sigma(\mathrm{AF})} \ , \tag{44}$$

which is always less than unity. The sign is chosen so that MR > 0 if the resistance increases with field, so our giant magnetoresistances are negative.

We show in Fig. 4 the conductivities of the various spin channels for a four-layer Fe-Cr-Fe-Cr sandwich structure, together with its resulting magnetoresistance. The MR is quite complicated, but arises from a fairly

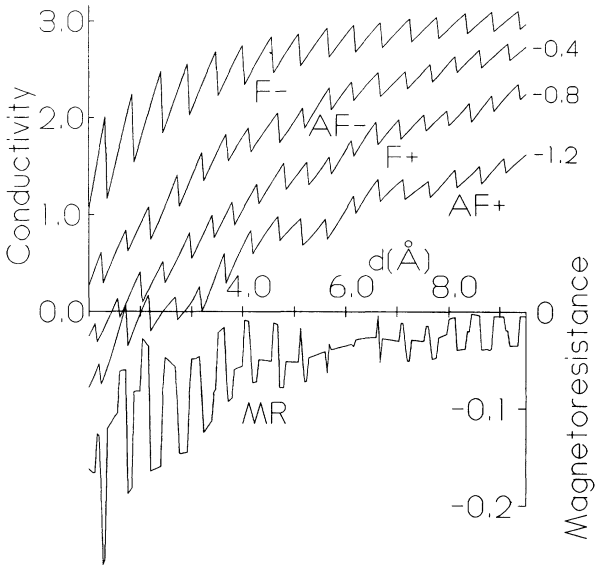

FIG. 4. Conductivities in a four-layer Fe-Cr-Fe-Cr sandwich, in the ferromagnetic state (curves labeled F+ and F− for up and down spin, respectively) and the antiferromagnetic state (curves labeled AF+ and AF−). Because the curves overlap heavily at large d, three of them have been displaced downward by 0.4, 0.8, and 1.2 units, as indicated. This does not change the order of the curves at most values of d; the minority (F−) conductivity is the largest. The scale at left uses a conductivity unit $e^2/8\pi^3 m$. The lowest curve is the magnetoresistance, whose scale is indicated at the right.

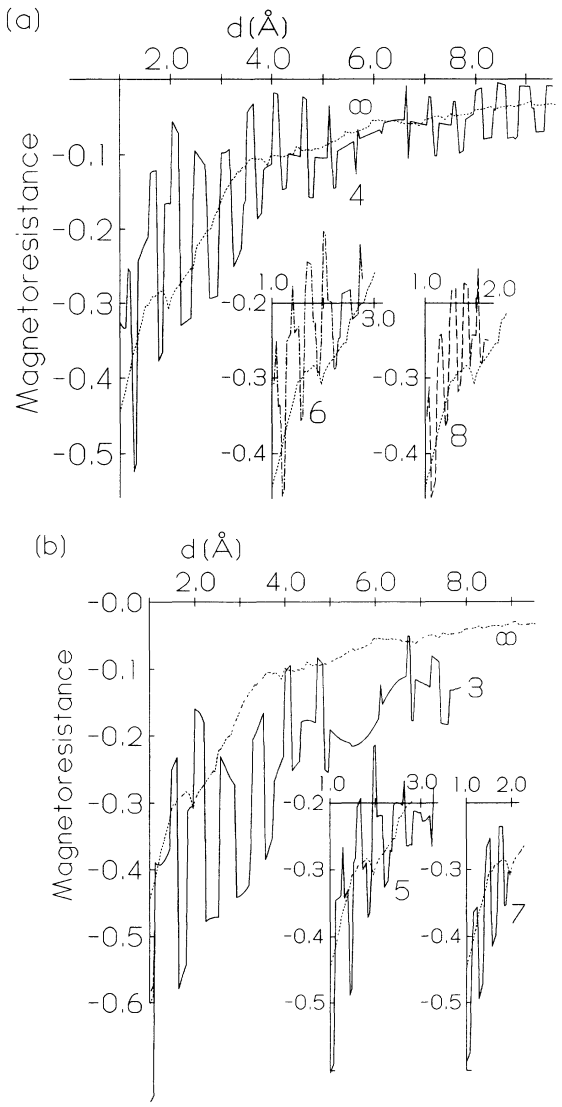

FIG. 5. (a) Magnetoresistances of FeCr sandwich structures with 4 (main graph), 6, and 8 (insets) layers. The dashed line superposed on each graph is the superlattice ($N=\infty$) result (Ref. 10). There are no data for large d and large N because when the total thickness $D=Nd$ is very large one encounters the overflow problems discussed in Sec. III. (b) MR for 3, 5, and 7 layers; these have one more Fe than Cr layer.

simple sawtooth pattern in the individual conductivities, involving a nearly linear rise followed by an abrupt drop. The drop is actually infinitely sharp in our model; the apparent width in Fig. 4 is due to the finite spacing of the sampled d's. The drop occurs when a new cylindrical piece of Fermi surface appears at small k_r, with area $dk_{FS}=(2\pi/D)(2\pi k_r)$. The corresponding extra density of final states [Eq. (27)] is $m/2\pi\hbar D$, *independently* of k_r. Thus the scattering rate [Eq. (32)] for all initial states increases discontinuously, and the relaxation time and conductivity decrease. An analogous (but not discontinuous) effect was seen[10] in the infinite superlattice, where such a conductivity decrease accompanies the appearance of a new lens sheet in the Fermi surface [such as that at the lower left in our Fig. 1(c)]. These quantum oscillations in MR should not be confused with the well-known oscillations in magnetic coupling[18] (we have assumed AF coupling for all layer spacings d) although the two phenomena are obviously closely related.

In spite of the complicated MR of the sandwich structure, it does appear to be consistent with convergence to the superlattice result[10] in the limit $N\rightarrow\infty$. We show in Fig. 5 the MR of sandwiches with various numbers N of layers, together with the $N=\infty$ result. Experimentally we expect the very rapid oscillations of MR with d that occur for large N to be smoothed out, giving a result very similar to the $N=\infty$ curve.

It is apparent from Figs. 4 and 5 that there is a long-period modulation of the MR oscillations due to beating between the conductivity oscillations in the various channels; this bears some resemblance to the aliasing effects that have been proposed as explanations of the long-period oscillations in antiferromagnetic coupling in layered systems.[19] Though the distance scale is sensitive to our choice of parameters (especially the itinerant-electron density), the period Δd of the present oscillations is so short that they are very likely to be washed out by layer-thickness fluctuations and therefore not experimentally observable.

VI. CONCLUSION

The transfer-matrix method makes it possible to calculate the electron wave functions in a model magnetic multilayer efficiently and rapidly enough that one can integrate over the Fermi surface and evaluate the conductivity, taking into account both bulk and interface (surface roughness) scattering. We find strong short-period quantum oscillations in the conductivities of sandwich structures. These oscillations may combine to produce long-period structure in the magnetoresistance. Similar effects have been found[10] for infinite superlattices.

TABLE II. Convergence of magnetoresistance of an infinite FeCr superlattice as the number of sampling points on the antiferromagnetic FS increases. (The number on each of the two ferromagnetic FS's is about $\frac{2}{3}$ of this.) Parameter values choices are those in Table I, with $d=2.2$ Å.

Convergence parameter Δ	Number of points	Magnetoresistance
0.1	37	0.27192
0.05	63	0.27848
0.025	125	0.27480
0.0125	242	0.27289
0.00625	458	0.27324
0.003125	915	0.27312

ACKNOWLEDGMENT

The author would like to thank Surrey University for its hospitality during the preparation of parts of this paper.

APPENDIX: CONVERGENCE WITH RESPECT TO NUMBER OF FERMI-SURFACE POINTS SAMPLED

In our program, the fineness of the Fermi-surface mesh is controlled by a dimensionless convergence parameter Δ. Roughly speaking, this is the fraction of each sheet of Fermi surface that is allowed to be represented by one point. More precisely, we require our increment dk_r to be less than $k_F\Delta$ (where k_F is an effective Fermi wave vector), the corresponding dk_z to be less than $2\pi\Delta/D$ and the number of points in each sheet to be more than Δ^{-1}. The convergence of the MR as $\Delta\rightarrow 0$ is given in Table II. It is not monotonic, because the MR is sensitive to the positioning of sample points with respect to the end points of FS sheets. However, at the value of $\Delta(0.0125)$ used in our figures it is quite well converged, to about 0.1%. The fractional uncertainty in MR is much greater for the case of spin-independent scattering,[10] because the MR itself is so much smaller, of order 2%. The uncertainty is especially large near the singularities at which a piece of FS first appears.

[1]M. N. Baibich, J. M. Broto, A. Fert, F. Dau, F. Petroff, P. Etienne, G. Creuzet, A. Friederich, and J. Chazelas, Phys. Rev. Lett. **61**, 2472 (1988).

[2]B. Dieny, V. S. Speriosu, S. Menin, S. S. P. Parkin, B. A. Gurney, P. Baumgart, and D. R. Wilhoit, J. Appl. Phys. **69**, 4774 (1991).

[3]D. Stoeffler and F. Gautier, Phys. Rev. B **44**, 10 389 (1991).

[4]K. Fuchs, Proc. Cambridge Philos. Soc. **34**, 100 (1938); H. Sondheimer, Adv. Phys. **1**, 1 (1952).

[5]R. E. Camley and J. Barnas, Phys. Rev. Lett. **63**, 664 (1989); J. Barnas, A. Fuss, R. E. Camley, P. Grünberg, and W. Zinn, Phys. Rev. B **42**, 8110 (1990).

[6]R. Q. Hood and L. M. Falicov, Phys. Rev. B **44**, 9989 (1991).

[7]F. Herman, J. Sticht, and M. van Shilfgaarde, in *Magnetic Thin Films, Multilayers, and Surfaces,* edited by S. S. P. Parkin, MRS Symposia Proceedings No. 231 (Materials Research Society, Pittsburgh, 1991).

[8]P. M. Levy and S. Zhang, Phys. Rev. Lett. **65**, 1643 (1990).

[9]P. M. Levy, Bull. Am. Phys. Soc. **37**, 683 (1992).
[10]P. B. Visscher and Hui Zhang, Phys. Rev. B **48**, 6672 (1993).
[11]R. de L. Kronig and W. G. Penney, Proc. R. Soc. London **A130**, 499 (1931).
[12]J. Inoue, A. Oguri, and S. Maekawa, J. Phys. Soc. Jpn. **60**, 376 (1991).
[13]J. Ziman, *Principles of the Theory of Solids* (Cambridge University Press, Cambridge, England, 1964), p. 182.
[14]In this spherical-symmetry case, it is a very simple linear functional, because the elastic-scattering assumption allows us to replace $g(k)$ by $g(k')$ and remove it from the integral. However, we do not exploit this here because it does not generalize to the cylindrical-symmetry case.
[15]E. Fermi, *Nuclear Physics* (University of Chicago Press, Chicago, 1950), p. 142.
[16]P. M. Levy, J. Magn. Magn. Mater. **121**, 357 (1993).
[17]J. Inoue, A. Oguri, and S. Maekawa, J. Phys. Soc. Jpn. **60**, 376 (1991).
[18]S. S. P. Parkin, N. More, and K. P. Roche, Phys. Rev. Lett. **64**, 2304 (1990).
[19]R. Coehorn, Phys. Rev. B **44**, 9331 (1991).